

Ferrimagnetism in delta chain with anisotropic ferromagnetic and antiferromagnetic interactions

D. V. Dmitriev and V. Ya. Krivnov*

*Institute of Biochemical Physics of RAS,
Kosygin str. 4, 119334, Moscow, Russia.*

(Dated:)

We consider analytically and numerically an anisotropic spin- $\frac{1}{2}$ delta-chain (sawtooth chain) in which exchange interactions between apical and basal spins are ferromagnetic and those between basal spins are antiferromagnetic. In the limit of strong anisotropy of exchange interactions this model can be considered as the Ising delta chain with macroscopic degenerate ground state perturbed by transverse quantum fluctuations. These perturbations lift the ground state degeneracy and the model reduces to the basal XXZ spin chain in the magnetic field induced by static apical spins. We show that the ground state of such model is ferrimagnetic. The excitations of the model are formed by ferrimagnetic domains separated by domain walls with a finite energy. At low temperatures the system is effectively divided into two independent subsystems, the apical subsystem described by the Ising spin- $\frac{1}{2}$ chain and the basal subsystem described by the XXZ chain with infinite zz interactions.

I. INTRODUCTION

The low-dimensional quantum magnets on geometrically frustrated lattices are extensively studied during last years [1, 2]. An important class of such systems is lattices consisting of triangles. An interesting and a typical example of these objects is the $s = \frac{1}{2}$ delta or the sawtooth Heisenberg model consisting of a linear chain of triangles as shown in Fig.1. The interaction J_1 acts between the apical (σ_i) and the basal (S_i) spins, while J_2 is the interaction between the neighboring basal spins. A direct interaction between the apical

*Electronic address: krivnov@deom.chph.ras.ru

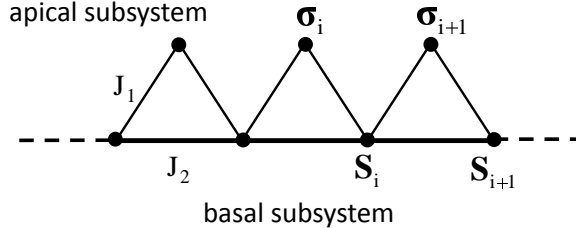


FIG. 1: The Δ -chain model.

spins is absent. The Hamiltonian of this model has a form

$$\begin{aligned} \hat{H} = & J_1 \sum_{i=1}^N [S_i^x(\sigma_i^x + \sigma_{i+1}^x) + S_i^y(\sigma_i^y + \sigma_{i+1}^y) + \Delta_1 S_i^z(\sigma_i^z + \sigma_{i+1}^z) - \frac{\Delta_1}{2}] \\ & + J_2 \sum_{i=1}^N [S_i^x S_{i+1}^x + S_i^y S_{i+1}^y + \Delta_2 (S_i^z S_{i+1}^z - \frac{1}{4})] \end{aligned} \quad (1)$$

where Δ_1 and Δ_2 are parameters representing the anisotropy of the basal-apical and the basal-basal exchange interactions respectively, N is the number of triangles. The constants in this equation are chosen so that the energy of the ferromagnetic state with the total spin $L_{tot}^z = S_{tot}^z + \sigma_{tot}^z = \pm N$ is zero.

The isotropic delta chain ($\Delta_1 = \Delta_2 = 1$) with both antiferromagnetic interactions $J_1 > 0$ and $J_2 > 0$ (AF delta chain) has been studied as a function of the parameter $\frac{J_2}{J_1}$ [3–5]. In spite of the simplicity of this model it exhibits a variety of peculiar properties. If $\frac{J_2}{J_1} = 1$ the model has two-fold degenerate ground state where neighboring pairs of spins form singlet configurations [4]. When $\frac{J_2}{J_1} = \frac{1}{2}$ the delta chain supports the independent localized magnon states. These states determine both the ground states properties and the low-temperature thermodynamics in the vicinity of the saturation magnetic field [6–10]. In particular, the ground state is highly degenerate, the zero-temperature magnetization has a plateau and the specific heat has the extra low-temperature peak.

In contrast to the AF delta chain the same model with $J_1 < 0$ and $J_2 > 0$ (the F-AF delta chain) is less studied. It is known [11] that the ground state of the F-AF isotropic delta chain is ferromagnetic for $\alpha = \frac{J_2}{|J_1|} < \frac{1}{2}$. It was argued in Ref.[11] on a base of numerical calculations that the ground state for $\alpha > \frac{1}{2}$ is a special ferrimagnetic state. The critical point $\alpha = \frac{1}{2}$ is the transition point between these two ground state phases. The isotropic F-AF delta-chain at the transition point $\alpha = \frac{1}{2}$ has been studied in Ref.[12]. It was shown [12] that the ground state at the transition point (at zero magnetic field) is macroscopically

degenerate and consists of multi-magnon configurations formed by independent localized magnons and the special localized multi-magnon complexes.

The isotropic F-AF delta chain is a minimal model for the description of several magnetic compounds such as malonato-bridged copper complexes of formula $[Cu(bpy)H_2O] \times [Cu(bpy)(mal)H_2O](ClO_4)_2$ containing magnetic Cu^{2+} ions [11, 13–15]. From the analysis of the experimental data it was concluded [13] that the ratio of exchange interactions $\alpha = \frac{J_2}{|J_1|}$ in this compound is $\alpha \simeq 1$. It means that this compound is on the ferrimagnetic side of the ground state diagram of the isotropic delta chain. Thus, the study of the ferrimagnetic state of the F-AF delta chain is important and interesting problem. Numerical calculations used in Ref.[11] suppose that the ground state magnetization per site in the ferrimagnetic phase in the isotropic model is $\frac{1}{4}$. Unfortunately, numerical methods do not allow to obtain the detail information about the structure and the properties of the ferrimagnetic phase. At the same time this model is rather complicated and can not be tractable analytically.

In this paper we show that the analysis of the anisotropic F-AF model in the limit of high anisotropy helps to understand the origin and the properties of the ferrimagnetic phase. For simplicity we consider the case of equal basal-apical and the basal-basal anisotropy $\Delta_1 = \Delta_2 = \Delta$. In this case with $\Delta \gg 1$ the ferrimagnetic phase can exist in a narrow interval of the value α (close to $\alpha = 1$) between the ferromagnetic (at $\alpha < \frac{\Delta}{1+\Delta}$) and the antiferromagnetic (at $\alpha > 1$) phases [14]. Therefore, in order to investigate the ferrimagnetic phase we put $\alpha = 1$. Then the Hamiltonian of the F-AF delta chain can be represented in a form:

$$\begin{aligned} \frac{1}{\Delta} \hat{H} = & \frac{1}{\Delta} \sum_{i=1}^N (S_i^x S_{i+1}^x + S_i^y S_{i+1}^y) - \frac{1}{\Delta} \sum_{i=1}^N [S_i^x (\sigma_i^x + \sigma_{i+1}^x) + S_i^y (\sigma_i^y + \sigma_{i+1}^y)] \\ & + \sum_{i=1}^N [S_i^z S_{i+1}^z - S_i^z (\sigma_i^z + \sigma_{i+1}^z) + \frac{1}{4}] \end{aligned} \quad (2)$$

where we put $J_1 = -1$ and $J_2 = 1$.

The main aim of this paper is to study the model (2) for $\Delta \gg 1$. We expect that some principal features of the ferrimagnetic phase of model (2) survive in the isotropic case.

Additional motivation of this study is related to the problem of ‘order by disorder’. The fact is that the model (2) in the limit $\Delta \rightarrow \infty$ turns into the classical Ising model on the delta chain with equal but opposite in sign apical-basal and basal-basal interactions:

$$\hat{H}_I = \sum_{i=1}^N [S_i^z S_{i+1}^z - S_i^z (\sigma_i^z + \sigma_{i+1}^z) + \frac{1}{4}] \quad (3)$$

It is known [16, 17] that the ground state of this model is macroscopically degenerate and it is separated from the excited states by a finite energy gap. This degenerate ground state is disordered (zero magnetization), and the main question of the ‘order by disorder’ problem is what happens when such disordered system is perturbed by the quantum fluctuations. The quantum fluctuations can lift the degeneracy and drive the system to either ordered or disordered ground state. Generally, there are many different ways of the introduction of such perturbations. One of them is given by the transverse terms in Eq.(2) and we will show that it leads to the ordered ground state. On the contrary, the perturbation of the Ising model (3) by a transverse magnetic field results in the disordered ground state [16].

Another example of influence of quantum dynamics on the Ising model (3) was considered in Ref.[17], where the anisotropic F-AF model (1) was studied for a special choice of the exchange interactions and the anisotropies: $\alpha = 1/(2\Delta_1)$ and $\Delta_2 = (2\Delta_1^2 - 1)$. For such choice of the interactions the F-AF model describes the phase boundary between different ground state phases on the (α, Δ_1) plane and reduces to the Ising model (3) at $\Delta_1 \rightarrow \infty$. The quantum fluctuations lift the ground state degeneracy of Ising model (3) but only partly, so that the degeneracy remains macroscopic on this phase boundary, it does not depend on Δ_1 and coincides with that for the isotropic F-AF delta-chain at $\alpha = \frac{1}{2}$. The spectrum of low-energy excitations has a highly nontrivial multi-scale structure leading to the specific low-temperature thermodynamics [17]. This special model is another example of ‘disorder by disorder’ instead of ‘order by disorder’.

The paper is organized as follows. In Section II we study the spectrum of model (2) in different sectors of total spin S_{tot}^z and show that the ground state is ferrimagnetic one. In Section III we study the low-temperature thermodynamics of the system both analytically and numerically. In Section IV we give a summary of our results.

II. FERRIMAGNETIC GROUND STATE

At $\Delta \rightarrow \infty$ the model (2) reduces to the Ising model on the delta-chain described by Hamiltonian (3). The total 4^N eigenstates of this model is divided in two subsets. The first one consists of degenerate ground states with zero energy. These states include two types of the spin configurations on triangles: either three spins in the triangle have the same orientation or two basal spins of the triangle are opposite oriented. In each triangle there

are three configurations which satisfy these conditions. Because the number of admissible configurations is the same for each triangle, the total number of the ground states is 3^N . $(4^N - 3^N)$ states of the second subspace are separated from the ground states by a ‘big’ gap with the energy $E \sim 1$.

An infinitesimal perturbation of transverse interactions in Eq.(2) lifts the macroscopic degeneracy of the ground state. However, a role of the first and the second terms in lifting is different. The first term has non-zero matrix elements both between the states of the first and the second subsets while the second term in Eq.(2) has non-zero matrix elements between the states of the first and the second subsets only. Thus, only the first term in Eq.(2) gives contributions to an energy to the first order in $\frac{1}{\Delta}$ whereas the second term is responsible for the corrections which are proportional to $\frac{1}{\Delta^2}$. Therefore, to the leading order in $\frac{1}{\Delta}$ we can neglect the second term in Eq.(2) and the Hamiltonian (2) reduces to that given by

$$\hat{H} = P[\Delta \hat{H}_I + \sum_{i=1}^N (S_i^x S_{i+1}^x + S_i^y S_{i+1}^y)]P \quad (4)$$

where P is a projector onto the first subspace containing 3^N states and $\Delta \rightarrow \infty$ is assumed.

The model (4) describes the basal XXZ chain with infinite zz interactions in the magnetic field produced by the static apical spins and the magnetic field in the i -th basal site is $h_i = \Delta(\sigma_i^z + \sigma_{i+1}^z)$. As a result, the magnetic field acting on the basal spins depends on the spin configuration of apical subsystem. At first we consider the most simple case when all apical spins are up (down) producing the uniform magnetic field on basal subsystem: $h_i = \Delta$ ($h_i = -\Delta$). It is easy to check that if all apical spins are up (down), the projector P in Eq.(4) eliminates the states in which two basal spins down (two spins up) occupy neighboring sites. The total number of allowable states is $(\frac{1+\sqrt{5}}{2})^N$ [18]. The Hamiltonian (4) for the case $h_i = \Delta$ takes the form

$$\hat{H} = P_0 \left\{ \sum_{i=1}^N (S_i^x S_{i+1}^x + S_i^y S_{i+1}^y) \right\} P_0 \quad (5)$$

where P_0 is the projector onto the states with no neighboring spins down.

The model (5) can be mapped onto spinless fermions via the Jordan-Wigner transformation

$$\begin{aligned} S_m^+ &= c_m^+ \exp(i\pi \sum_{l>m} c_l^+ c_l) \\ S_m^z &= \frac{1}{2} - c_m^+ c_m \end{aligned} \quad (6)$$

where c_m^+ is the Fermi-operator and we identify a spin down and a spin up as a particle and a hole, correspondingly.

In fermion language the Hamiltonian (5) reads

$$\hat{H} = P_0 \left\{ \frac{1}{2} \sum_{i=1}^N (c_i^+ c_{i+1} + c_{i+1}^+ c_i) \right\} P_0 \quad (7)$$

and the projector P_0 forbids two particles to occupy neighboring sites.

The model of the spinless fermions with such constraint (infinite nearest-neighbor interaction) can be mapped onto the model of non-interacting fermions as follows [19] (for simplicity, we consider an open chain with N sites). Each configuration of M fermions on N sites with constraint is mapped to the configuration of M fermions on $(N - M + 1)$ sites without constraint by removing one empty site between two occupied sites. The Hamiltonian of such model depends on a number of fermions and has a form

$$\hat{H}(M) = \frac{1}{2} \sum_{i=1}^{N-M+1} (c_i^+ c_{i+1} + c_{i+1}^+ c_i) \quad (8)$$

Besides, the matrix elements between the corresponding configurations of Eq.(7) and Eq.(8) are equal to each other. An equivalence of two models means that the dispersion relation in the spin sector $S^z = \frac{N}{2} - M$ is

$$\varepsilon(k_m) = -\cos k_m \quad (9)$$

where

$$k_m = \frac{\pi m}{N - M + 2} \quad (10)$$

with $m = 1, 2, \dots, N - M + 1$.

According to Eq.(9) the ground state energy of model (8) in the limit $N, M \gg 1$ but for a fixed fermion density $\rho = \frac{M}{N}$ is

$$E_0(\rho) = N \frac{1 - \rho}{\pi} \sin \left(\frac{\pi \rho}{1 - \rho} \right) \quad (11)$$

Minimization of $E_0(\rho)$ with respect to ρ gives

$$\rho = \rho_0 \simeq 0.3008 \quad (12)$$

and

$$E_0(\rho_0) \simeq -0.217N \quad (13)$$

Returning to the spin language, Eq.(12) means that the ground state of Eq.(5) is realized in the spin sector $S^z = N(\frac{1}{2} - \rho_0)$. Thus, the total spin of the ground state of delta chain (2) is

$$L_z^z = N(1 - \rho_0) \quad (14)$$

It follows from Eq.(11) that the energy of the lowest excitations in this spin sector is

$$\varepsilon = \frac{\pi(1 - \rho_0)}{N} \sin\left(\frac{\pi\rho_0}{1 - \rho_0}\right), \quad (15)$$

i.e. the excitations are sound-like with the sound velocity

$$c = \sin\left(\frac{\pi\rho_0}{1 - \rho_0}\right) \quad (16)$$

The case with all apical spins down is considered in a similar way. In this case the role of the Fermi-particles is played by the basal spins up and the total ground state spin is $L_z^0 = -N(1 - \rho_0)$.

We note that formulae similar to Eqs.(11) and (12) have been obtained earlier by the Bethe-ansatz method [20] in the problem of an asymmetric diffusion of molecules with different size.

Eq.(11) with $\rho = \rho_0$ defines the ground state energy of the Hamiltonian (4) for the ferromagnetic configuration of the apical subsystem. Now we need to consider other distributions of up and down apical spins. This problem can not be solved analytically and we use numerical calculations of finite chains. These calculations show that the most important configurations of the apical spin subsystem are the states with alternating domains of the up and down spins. The simplest configuration of such type is a two-domain structure consisting of l spins up and $(N - l)$ spins down separated by two domain walls (for cyclic chains). For the two-domain configuration the magnetic field induced by the apical spins is: $h = \Delta$ for $(l - 1)$ basal sites; $h = -\Delta$ for $(N - l - 1)$ sites; and $h = 0$ on two basal sites located in the center of two domain walls. (The ferromagnetic state of the apical spins considered above corresponds to $l = 0$ or $l = N$ and it can be identified as the one-domain structure). It is apparent that the minimal energy of the two-domain state with $l, N \gg 1$ is reached when the density of the fermions (in fermionic language) in each domain is $\rho = \rho_0$. The total spin of this state is $L^z = (2l - N)(1 - \rho_0)$. It is clear that the energy of this state is higher than the ground state energy of the one-domain state due to the presence of defects (the domain walls). The energy of the domain wall $E_{dw}(l)$ is defined as a half of the energy difference

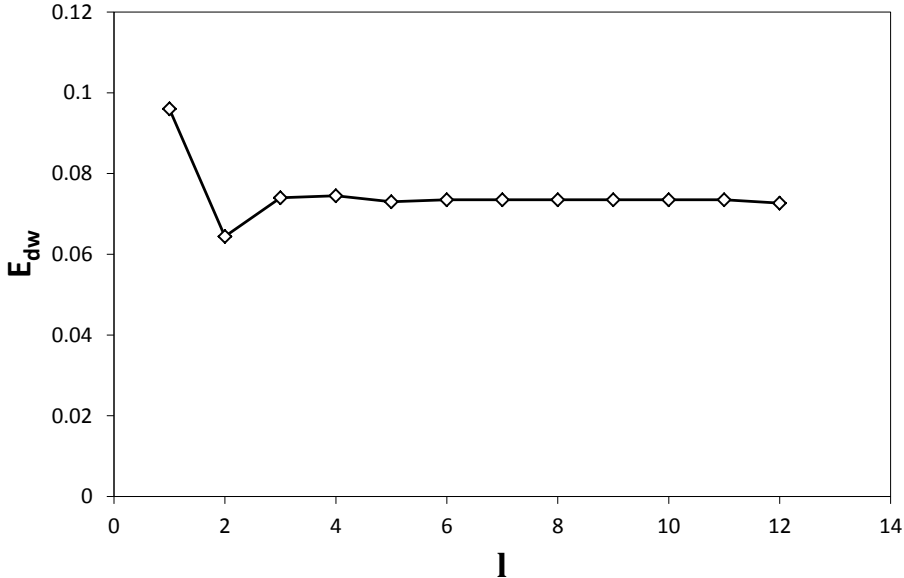


FIG. 2: Dependence of the domain wall energy on the domain size $E_{\text{dw}}(l)$ is calculated for the cyclic XXZ chain of length $N = 24$ as a half of the energy difference between the two-domain configuration with l apical spins down and $(N - l)$ apical spins up and the one-domain ground state energy.

between the two-domain configuration with l apical spins down and $(N - l)$ apical spins up and the one-domain ground state energy. The numerical calculations on finite chain $N = 24$ for the dependence of the domain wall energy on the domain size $E_{\text{dw}}(l)$ are shown in Fig.2. The energies of the one-domain and two-domain states are chosen for the optimal value of the total S^z . As can be seen in Fig.2 the domain wall energy E_{dw} slowly depends on l when the domain size $l \geq 2$ and $N \gg 1$ and rapidly converges to the value $E_{\text{dw}} \simeq 0.07$.

Similarly, any apical spin configuration can be represented as many domain structure consisting of r domains with spins up and r domains with spins down domains with $2r$ domain walls. Numerical calculations show that the ground state energy of the r -domain state is

$$E(r) = E_0 + 2rE_{\text{dw}} \quad (17)$$

where E_0 is the ground state energy of the one-domain configuration ($r = 0$) given by Eq.(11).

In order to study the stability of the one-domain ground state with respect to a creation of the two-domain states we consider the dependence of the ground state of the one-domain configuration with all apical spins up, $E_0(\rho)$, for ρ close to ρ_0 . According to Eq.(11) the

energy $E_0(\rho)$ has a minimum at ρ_0 and can be expanded in $|\rho - \rho_0| \ll 1$ as

$$E_0(\rho) = E_0(\rho_0) + bN(\rho - \rho_0)^2 \quad (18)$$

where

$$b = \frac{\pi}{2(1 - \rho_0)^3} \sin\left(\frac{\pi\rho_0}{1 - \rho_0}\right) \approx 4.46 \quad (19)$$

In an instability point the energies and the total spins of the one- and two-domain states are equal. The total spins of the one-domain state and two-domain one with l up and $(N-l)$ down apical spins are $L^z = N(1 - \rho)$ and $L^z = (N - 2l)(1 - \rho_0)$, respectively. As a result the instability point is determined by the relations

$$\begin{aligned} bN(\rho - \rho_0)^2 &= 2E_{\text{dw}} \\ (\rho - \rho_0) &= 2\left(1 - \frac{l}{N}\right)(1 - \rho_0) \end{aligned} \quad (20)$$

As follows from Eqs.(20) the instability occurs for $\rho > \rho_0$ and for small deviation from the minimum $(\rho - \rho_0) \sim N^{-1/2}$. Thus, in the thermodynamic limit $N \rightarrow \infty$ the ground state is realized for the one-domain state in the total spin sectors with $|L^z| \geq L_0^z$ (see Eq.(14)), while in the sectors $|L^z| < L_0^z$ the ground state corresponds to the two-domain structure. But the global ground state of the model (4) is twofold degenerate ferrimagnetic state with $L^z = \pm L_0^z$. In these states the magnetization on apical and basal sublattices are $|\langle \sigma_i^z \rangle| = 0.5$ and $|\langle S_i^z \rangle| \simeq 0.2$, so that the total magnetization per site is $|\langle \frac{L^z}{2N} \rangle| = 0.35$. The ground state energy as a function of L^z/N obtained by numerical calculations of finite delta-chains with $N = 10$ and $N = 14$ is shown in Fig.3. Irregular form of this dependence is due to finite-size effects, which are caused mainly by the deviation of the particle density $\rho = M/N$ possible for a given chain length N from the optimal value ρ_0 . However, as it can be seen in Fig.3 the amplitude of oscillations decreases with N and the expected thermodynamic limit $2E_{\text{dw}}$ is shown in Fig.3 by thick solid line.

III. LOW TEMPERATURE THERMODYNAMICS

The partition function Z of the model (4) is a sum of contributions to Z corresponding to all possible configurations of the apical spins. Generally, each configuration of the cyclic delta-chain with $2r$ domain walls is specified by a set of r domains of the apical spins up with

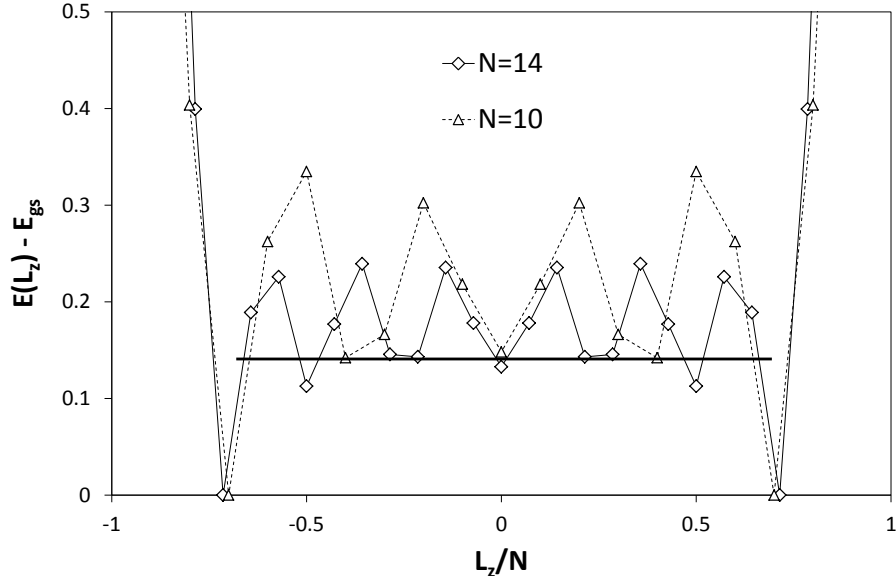


FIG. 3: Lowest energies in different sectors of total spin L_{tot}^z for delta-chains with $N = 10$ and $N = 14$. Predicted thermodynamic limit is shown by thick solid line.

lengths l_1, l_2, \dots, l_r and r domains of the apical spins down of length m_1, m_2, \dots, m_r which satisfy the conditions

$$\sum_{i=1}^r l_i = N - k, \quad \sum_{i=1}^r m_i = k \quad (21)$$

where k is a total number of down apical spins.

Then, the partition function Z is

$$Z = \sum_r Z_r(l_1, m_1, l_2, m_2, \dots, l_r, m_r) \quad (22)$$

where summation is carried out over l_i, m_i satisfying relations (21) and it includes two one-domain configurations with $r = 0$.

The calculation of Z in Eq.(22) is a complicated problem. However, it can be simplified for low temperatures. As was noted before the ground state energy of the configurations with $2r$ domain walls is higher than the one-domain state on the value $2rE_{dw}$. The same holds for the free energies. As an example, we represent in Fig.4 the difference between the free energies of the one-domain ($r = 0$) and two-domain ($r = 1$) configurations of cyclic chain with $N = 8$ as the function of T . This difference varies only slightly with T and it is close to the energy of two domain walls $2E_{dw}$, so that the deviation from the value $2E_{dw}$ is less than 7% for $T < T_1 \simeq 0.5$. It means that the two-domain partition function Z_1 at

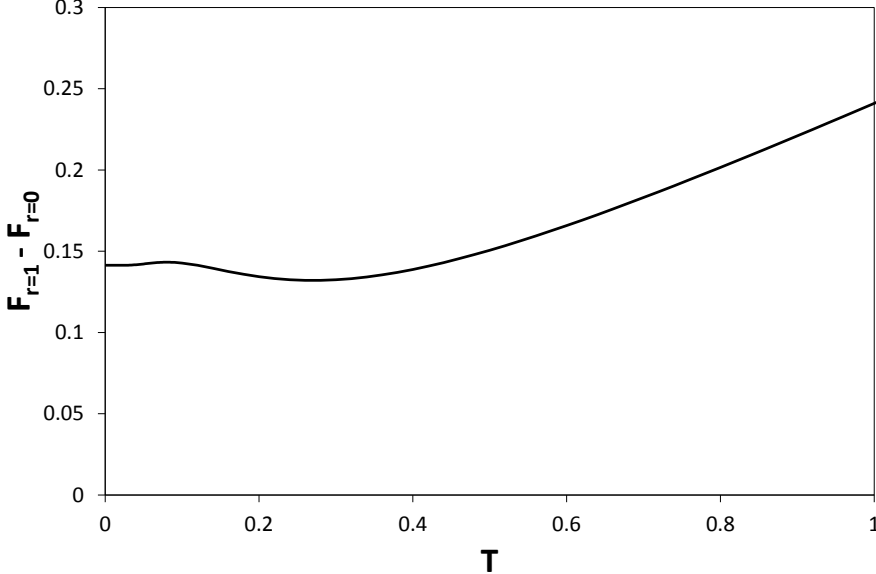


FIG. 4: Difference of the free energies of the two-domain ($r = 1$) and the one-domain ($r = 0$) configurations as a function of T for the XXZ chain of length $N = 16$.

$T < T_1$ can be written as

$$Z_1 = Z_0 \exp\left(-\frac{2E_{\text{dw}}}{T}\right) \quad (23)$$

where Z_0 is the partition function of the model (5) describing the one-domain configuration.

Similarly, if all domain sizes are large ($l_i, m_j \gg 1$), the free energy per site is the same for each domain and it is equal to that for the one-domain configuration. Therefore, the partition function of the r - domain configuration can be approximately written as

$$Z_r = Z_0 \exp\left(-2r\frac{E_{\text{dw}}}{T}\right) \quad (24)$$

Then the partition function (22) takes the form

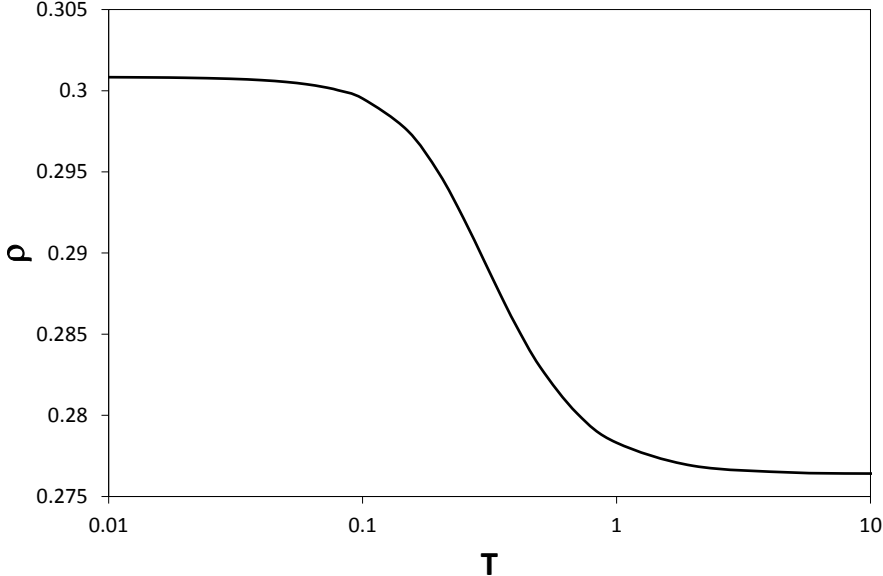
$$Z = Z_0 \sum_{r=0}^{N/2} \exp\left(-2r\frac{E_{\text{dw}}}{T}\right) W(r, N) \quad (25)$$

where $W(r, N)$ for $r \geq 1$ is the number of the configurations with $2r$ domain walls. The weights $W(r, N)$ are known [21]

$$W(r, N) = \sum_{m=r}^{N-r} \frac{N}{m} C_m^r C_{N-m-1}^{r-1} \quad (26)$$

where C_n^k are binomial coefficients and $W(0, N) = 2$.

The sum in Eq.(25) looks like the partition function of the 1D Ising model of the apical spins $\sigma = \frac{1}{2}$ with the effective nearest-neighbor ferromagnetic interaction $J = E_{\text{dw}}$, i.e. the

FIG. 5: Dependence $\rho(T)$.

partition function Z at $T < T_1$ is a product of the partition functions of the model (5) and that of the effective 1D Ising model Z_I , i.e $Z = Z_0 Z_I$. It means that the free energy and other thermodynamic quantities are sums of those for the 1D Ising model and for the model (5). As to the thermodynamics of the latter it can be obtained using the known spectrum of this model given by Eq.(9). Then, the free energy $F_0 = -T \ln Z_0$ has a form

$$\frac{F_0}{N} = -\frac{T(1-\rho)}{\pi} \int_0^\pi \ln[1 + \exp(\frac{\cos k + \mu}{T})] dk \quad (27)$$

The chemical potential μ and the density ρ as functions of T are determined from the equations $\partial F/\partial \rho = 0$ and $\partial F/\partial \mu = 0$ with $F = F_0 + \mu \rho$, which result in

$$\begin{aligned} \mu &= -\frac{T}{\pi} \int_0^\pi \ln[1 + \exp(\frac{\cos k + \mu}{T})] dk \\ \rho &= \frac{(1-\rho)}{\pi} \int_0^\pi [1 + \exp(-\frac{\cos k + \mu}{T})]^{-1} dk \end{aligned} \quad (28)$$

In particular, the temperature dependence of the density $\rho(T)$ is shown in Fig.5. As follows from Fig.5 $\rho(T)$ changes from $\rho \simeq 0.3$ at $T = 0$ to $\rho = (\sqrt{5} - 1)/2\sqrt{5} \simeq 0.276$ at $T \gg 1$. The formula (27) coincides with that obtained by different method in Ref.[22], where the XXZ chain in the vicinity of the triple point has been studied.

Using Eq.(27) and well known thermodynamics of the 1D Ising model we can obtain all thermodynamic quantities of the model (4). As an example, the specific heat $C(T) = C_I(T) + C_0(T)$ as a function of T is shown in Fig.6 together with the contributions $C_I(T)$

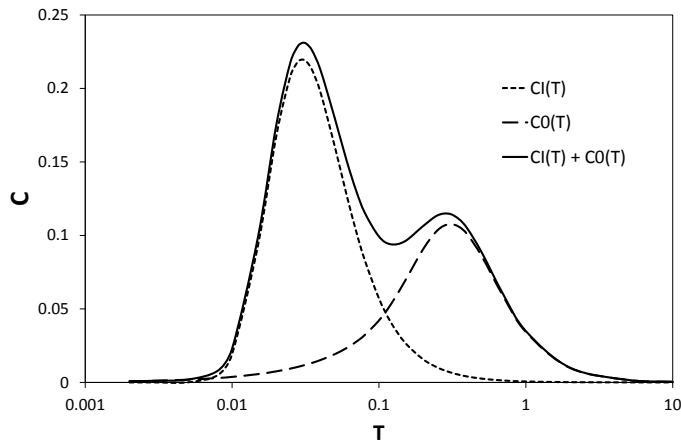


FIG. 6: Two contributions to the specific heat and their sum as a function of T .

and $C_0(T)$. The specific heat has a sharp maximum at $T \simeq 0.03$ and the main contribution to it is given by the Ising term, while the shoulder in $C(T)$ at $T \simeq 0.3$ is related to the maximum in $C_0(T)$. At $T \rightarrow 0$ the ‘Ising’ contribution $C_I(T)$ is exponentially small and the specific heat is uniquely determined by that for $C_0(T)$

$$\frac{C}{N} = 2(1 - \rho_0)\pi T \sin^{-1}\left(\frac{\pi\rho_0}{1 - \rho_0}\right), \quad T \rightarrow 0 \quad (29)$$

As we noted before, Eqs. (24) and (25) are valid when the domain sizes in the many domain configurations are large. To determine the temperature region for which this is the case we use the steepest descent method for the calculation of the sum in Eq.(25). Using Stirling’s formula for the binomial coefficients in $W(r, N)$ we found that the main contribution to the sum is given by the terms with

$$\begin{aligned} k &= \frac{N}{2} \\ r &= \frac{N}{2}\left(1 + \exp\left(\frac{E_{\text{dw}}}{T}\right)\right)^{-1} \\ l_{\downarrow} &= l_{\uparrow} = \left(1 + \exp\left(\frac{E_{\text{dw}}}{T}\right)\right) \end{aligned} \quad (30)$$

where l_{\uparrow} and l_{\downarrow} are average lengths $\langle l_i \rangle$ and $\langle m_j \rangle$ of up- and down domains.

According to Eq.(30) the representation of the partition function in the form (25) is valid if $\exp(E_{\text{dw}}/T) \gg 1$ (or $T < E_{\text{dw}}$). Because $E_{\text{dw}} < T_1$ we conclude that the partition function in the form (25) secures a correct thermodynamics of the model (4) for $T < E_{\text{dw}}$, while for $T > E_{\text{dw}}$ it can give a qualitative description only.

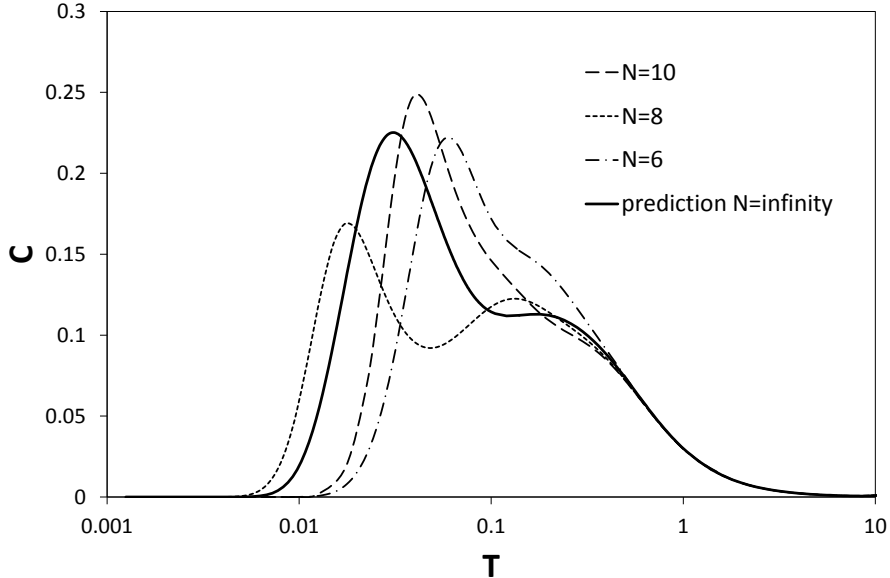


FIG. 7: Specific heat $C(T)$ calculated for delta chains with $N = 6, 8, 10$ and that predicted by approximation (32).

Nevertheless, our calculations of finite systems show that all r - dependence of the partition function $Z_r(l_1, m_1, l_2, m_2, \dots, l_r, m_r)$ for the configurations with small domains is expressed by the factor $\exp(-2rE_{\text{dw}}/T)$ where $E_{\text{dw}} \simeq 0.07$ as before. According to Eq.(30) for $T > E_{\text{dw}}$ the average size of domains becomes $l_\downarrow = l_\uparrow \simeq 2$. Using these facts we take as an approximation for the r - domain partition function $Z_r(l_1, m_1, l_2, m_2, \dots, l_r, m_r)$ the expression in a form

$$Z_r = \tilde{Z} \exp(-2r \frac{E_{\text{dw}}}{T}) \quad (31)$$

where \tilde{Z} is the partition function for the up-up-down-down ($\uparrow\uparrow\downarrow\downarrow\uparrow\uparrow\downarrow\downarrow\dots$) configuration of the apical spins.

Then, the partition function Z at $T > E_{\text{dw}}$ is

$$Z = \tilde{Z} Z_I \quad (32)$$

The thermodynamics of the up-up-down-down configuration is found by an exact diagonalization (ED) calculation of finite chains. Corresponding results for the specific heat are presented in Fig.7. In Fig.7 we also represent the results of the ED calculations of the model (2) with $\Delta = 100$ for $N = 6, 8, 10$. We note that the model (2) with large but finite Δ and the model (4) are formally non-equivalent because the total number of states of these two models are different and include 4^N and 3^N states, respectively. However, in the temperature region $T < 10$ the thermodynamics of the model (2) is governed by exactly 3^N states

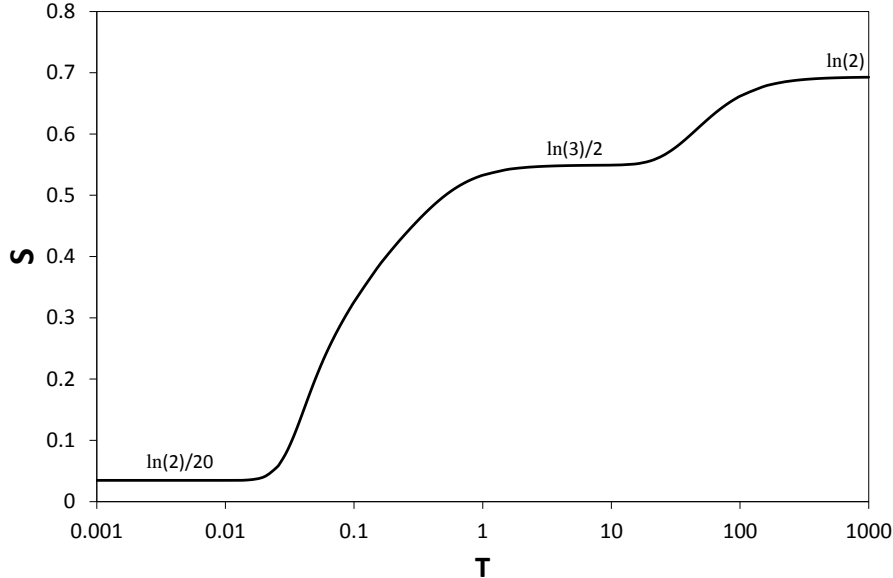


FIG. 8: Dependence of entropy per site on temperature $S(T)$ for model (2) with $\Delta = 100$ and $N = 10$.

as follows from the temperature dependence of the entropy per spin (see Fig.8). Thus, at $T < 10$ the thermodynamics of the models (4) and (2) is identical. As it can be seen in Fig.7, the data for $C(T)$ for the model (2) with different N deviate at $T \lesssim E_{\text{dw}}$ both from each other and from the results for infinite system obtained from Eq.(25). It means that the finite-size effects are essential in this temperature region. On the other hand, the data for different N are indistinguishable at $T \gtrsim 1$, testifying that the finite-size data correctly describe the thermodynamic limit. We note also that at $T \gtrsim 1$ these data are close to those obtained from Eq.(31) for the up-up-down-down configuration. At the same time, the thermodynamics based on Eqs.(25) show the qualitatively similar behavior of the specific heat in this temperature region.

Lastly, we consider the temperature dependence of the zero-field susceptibility $\chi(T)$. In this case it is necessary to include the external magnetic field $h_{\text{ext}} \ll 1$ in the model (2). We confine ourself by the temperature region $T \lesssim E_{\text{dw}}$ where the partition function is the product of the Ising and the one-domain terms. We do not dwell on the technical details of the corresponding computations. They are related to the solutions of Eqs.(27) and (28) as the functions of the temperature and the magnetic field h_{ext} . The final result for the zero-field susceptibility $\chi(T)$ has the form

$$\frac{\chi(T)}{N} = 2\chi_I(T)(1 - \rho(T)) + \chi_0(T) \quad (33)$$

where $\chi_I(T)$ is the zero-field susceptibility per site of the above-mentioned effective Ising model:

$$\chi_I = \frac{1}{4T} \exp\left(-\frac{E_{\text{dw}}}{2T}\right) \quad (34)$$

$\rho(T)$ is the solution of Eq.(28) with $h_{\text{ext}} = 0$ and $\chi_0(T)$ is the susceptibility of the model (5) given by

$$\chi_0(T) = \frac{(1 - \rho(T))^3}{\pi T} \int_0^\pi \exp\left(-\frac{\cos k + \mu(T)}{T}\right) [1 + \exp\left(-\frac{\cos k + \mu(T)}{T}\right)]^{-2} dk \quad (35)$$

with $\mu(T)$ determined by Eq.(28) with $h_{\text{ext}} = 0$.

The temperature dependence of the quantity $\chi(T)T$ is shown in Fig.9. The susceptibility χ_I is proportional to $\frac{1}{T} \exp(E_{\text{dw}}/2T)$ at $T \rightarrow 0$ while $\chi_0(0)$ is finite

$$\chi_0(0) = \frac{(1 - \rho_0)^3}{\pi \sin\left(\frac{\pi \rho_0}{1 - \rho_0}\right)} \quad (36)$$

Therefore, the behavior of the susceptibility at low temperatures is determined by the ‘Ising’ contribution χ_I and, therefore, exponentially diverges at $T \rightarrow 0$. In Fig.9 we also represent the temperature dependence of $\chi(T)T$ for finite delta-chains obtained by the ED calculations of model (2). In contrast to the analytics predicting the exponentially divergence of $\chi(T)T$ in the thermodynamic limit, the calculations of finite chains show the finite limit for $\chi(T)T$ at $T = 0$. Such behavior is related to the fact that the value $\chi(T)T$ at $T = 0$ for finite N equals to the square of the ground state spin which is $L_z^2 = N^2(1 - \rho_0)^2$, which turns into the divergence of $\chi(T)T$ in the thermodynamic limit.

IV. SUMMARY

We have studied the spin- $\frac{1}{2}$ F-AF delta chain in the limit of large anisotropy of exchange interactions. In this limit the model reduces to the 1D XXZ chain on basal sites in the static magnetic field depending on the domain structure of the apical spins. The ground state is twofold degenerate and magnetically ordered. In the ground state the apical spins form a fully polarized state with $|\langle \sigma_i^z \rangle| = 0.5$ and the magnetization of the basal spins is $|\langle S_i^z \rangle| \simeq 0.2$. Of particular interest are the excited states which involve the domain walls separating the domains of one or another ground state. Based on the domain statistics we reduced the low-temperature thermodynamics problem to those for the effective 1D Ising model for the apical subsystem and the 1D XXZ chain with infinite zz interactions for the

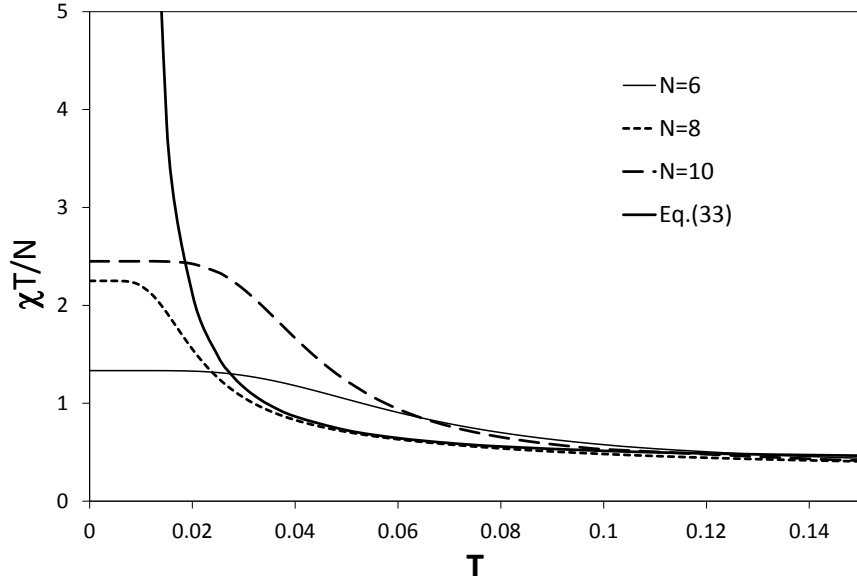


FIG. 9: Dependence of the susceptibility per site $\chi(T)T/N$ on T for model (4) with $N = 6, 8, 10$. Analytical prediction Eq.(33) is shown by thick solid line.

basal subsystem. The correlation functions $\langle \sigma_i^z \sigma_{i+r}^z \rangle$ and $\langle S_i^z S_{i+r}^z \rangle$ behave similarly to 1D Ising ones with a correlation length proportional to $\exp(E_{\text{dw}}/2T)$ at low temperatures.

This simple picture provides a starting point for the qualitative understanding of the ferrimagnetic phase of the isotropic model. Preliminary numerical results indicate that the ground state magnetization on the apical and the basal sites does not change considerably when the anisotropy parameter Δ decreases from the large value to 1. In the isotropic case they are $\langle \sigma_i^z \rangle = 0.414$ and $\langle S_i^z \rangle = 0.086$ [23]. However, additional symmetry of the isotropic model requires certain modifications of the presented approach.

Acknowledgments

We would like to thank J.Richter for valuable comments on the manuscript. The numerical calculations were carried out with use of the ALPS libraries [24].

[1] H. T. Diep, ed., *Frustrated spin systems* (World Scientific, Singapore, 2013).
 [2] C. Lacroix, P. Mendels and F. Mila, eds., *Introduction to frustrated magnetism. Materials, Experiments, Theory* (Springer-Verlag, Berlin, 2011).

- [3] D. Sen, B.S. Shastry, R.E. Walstedt and R. Cava, Phys. Rev. B **53**, 6401 (1996).
- [4] T. Nakamura and K. Kubo, Phys. Rev. B **53**, 6393 (1996).
- [5] S. A. Blundell and M. D. Nuner-Reguerio, Eur. Phys. J. B **31**, 453 (2003).
- [6] O. Derzhko, J. Richter, M. Maksymenko, Int. J. Modern Phys. **29**, 1530007 (2015).
- [7] M. E. Zhitomirsky and H. Tsunetsugu, Phys. Rev. B **70**, 100403 (2004).
- [8] J. Schnack, H.-J. Schmidt, J. Richter and J. Schulenburg, Eur. Phys. J. B **24**, 475 (2001).
- [9] J. Richter, J. Schulenburg, A. Honecker, J. Schnack, and H.J. Schmidt, J. Phys.: Condens. Matter **16**, S779 (2004).
- [10] O. Derzhko and J. Richter, Phys. Rev. B **70**, 104415 (2004).
- [11] T. Tonegawa and M. Kaburagi, J. Magn. Magn. Materials, **272**, 898 (2004).
- [12] V. Ya. Krivnov, D. V. Dmitriev, S. Nishimoto, S.-L. Drechsler, and J. Richter, Phys. Rev. B **90**, 014441 (2014).
- [13] Y. Inagaki, Y. Narumi, K. Kindo, H. Kikuchi, T. Kamikawa, T. Kunimoto, S. Okubo, H. Ohta, T. Saito, H. Ohta, T. Saito, M. Azuma, H. Nojiri, M. Kaburagi and T. Tonegawa, J. Phys. Soc. Jpn. **74**, 2831 (2005).
- [14] M. Kaburagi, T. Tonegawa and M. Kang, J.Appl.Phys. **97**, 10B306 (2005).
- [15] C. Ruiz-Perez, M. Hernandez-Molina, P. Lorenzo-Luis, F. Lloret, J. Cano, and M. Julve, Inorg. Chem. **39** 3845 (2000).
- [16] R. Moessner and S. L. Sondhi, Phys. Rev. B **63**, 224401 (2001).
- [17] D. V. Dmitriev, V. Ya. Krivnov, Phys. Rev. B **92**, 184422 (2015).
- [18] C. Domb, Adv. Phys. **9**, 149 (1960).
- [19] S. -A. Cheong and C. L. Henley, Phys. Rev. B **80**, 165124 (2009).
- [20] F. C. Alcaraz and R. Z. Bariev, Phys. Rev. E **60**, 79 (1999); cond-mat/9904042.
- [21] M. Gaudin, The Bethe wave function, Cambridge University Press, 2014.
- [22] C. Trippe, F. Gohman, and A. Klumper, cond-mat/0912.1739.
- [23] S. Nishimoto, S.-L. Drechsler, and J. Richter, private communications.
- [24] B. Bauer et al., J. Stat. Mech. P05001 (2011).